

# Bias free magnetomechanical coupling on magnetic microwires for sensing applications

C. Herrero-Gómez,<sup>a)</sup> P. Marín, and A. Hernando

*Departamento de Física de Materiales, Instituto de Magnetismo Aplicado, Universidad Complutense de Madrid-CSIC-ADIF, P.O. Box 155, Las Rozas, Madrid 28230, Spain*

(Received 29 July 2013; accepted 4 September 2013; published online 3 October 2013)

In the present paper, we report a systematic study of the magnetoelastic resonance of amorphous magnetic microwires of composition  $Fe_{73}Si_{11}B_{13}Nb_3$ . The study was performed for samples annealed at different temperatures. It was observed that such microwires present the key feature of performing magnetoelastic resonance in the absence of applied field. This fact, in addition to their small size, gives the microwires unique advantages over the widespread ribbons, currently in use as magnetoelastic sensors. Beyond the study of the resonance, magnetic properties of the samples were studied by means of Vibrating Sample Magnetometer (VSM) measurement in order to find an explanation to their bias-free resonance property. Finally, we show two possible applications of microwire based magnetoelastic sensors, a fluid density sensor and a mass-loading sensor. © 2013 AIP Publishing LLC. [<http://dx.doi.org/10.1063/1.4821777>]

In recent years, much interest and effort has been devoted to develop soft magnetic materials due to their technological potential.<sup>1</sup> The main use of these materials can be found in the sensing industry which includes a broad spectrum of applications ranging from the automotive, mobile communication, chemistry and biochemistry industry among many others.<sup>2–5</sup>

Amorphous microwires are one of the most widely studied soft materials. They are fabricated by means of extracting melt-spinning Taylor technique.<sup>6</sup> Those microwires are composed by a metallic core and a Pyrex cover both in the  $\mu\text{m}$  range. The metallic core provides the magnetic behaviour while the cover has a protective and stress-inducing function.<sup>7</sup> The ratio between the total diameter and the magnetic core, often called aspect ratio, is one of the key parameters of such microwires, since magnetic properties depend dramatically on it. For high values of the aspect ratio, the microwires present a bistable hysteresis loop, while this bistability vanishes for low ones.<sup>8,9</sup> In fact, amorphous or nanocrystalline magnetic microwires are among the softest materials. Many properties of these materials have been deeply studied both from the point of view of the basic physics and the applications.<sup>10,11</sup> This is the case of the giant magnetoimpedance effect,<sup>12</sup> biestability,<sup>13</sup> and ferromagnetic resonance.<sup>14</sup> However, the magnetoelastic resonance of those materials was only thoughtfully considered a few years ago.<sup>15</sup>

It is well known that amorphous magnetostrictive alloys present magnetoelastic nature, so those materials may perform magnetoelastic resonance when exposed to a time-varying magnetic field. The physical parameters that describe this resonance, such as the resonance frequency, the amplitude, and the damping, are functions of the material environment. For this reason, their monitorization may be used to obtain information about the media. That is the working principle of a magnetoelastic sensor.<sup>16–19</sup> This kind of sensors allow a high degree of specificity, by functionalizing the sensing material to make it react with an specific agent of

the media, as can be certain gases (e.g., humidity<sup>20</sup> or  $CO_2$  sensors,<sup>21</sup>), chemical or biological agents (pH,<sup>22</sup> blood coagulation,<sup>23,24</sup> lipoproteins,<sup>25</sup>) and stress,<sup>26</sup> or viscosity sensors.<sup>27</sup> Their versatility and the fact of being interrogated without physical contacts, make those sensors very suitable and useful for several applications in different fields.

In this context, ribbon-shaped magnetoelastic sensors of amorphous iron-based composition as METGLAS have become the most popular ones, and considerable work has been done in order to improve their magnetoelastic behaviour and sensor performance. The latter was achieved by different techniques. Among all, heat annealing under transverse magnetic field is the one that leads the best results.<sup>28</sup> Moreover, they have already been used in industry for many applications, such as magnetic tags, or commercial sensors with a high level of commercial acceptance. However, a common feature of the ribbon-based magnetoelastic sensors is that they all need a DC bias field to operate (i.e., to perform magnetoelastic resonance). This field is usually supplied by either a bias coil or by a hard magnet. The need of such a bias element increases drastically the size of those magnetoelastic sensors, being an important drawback for their miniaturization.

A step further was taken by Marín *et al.*<sup>15</sup> with the development of a magnetoelastic sensor based in an amorphous magnetic microwire, which was proved to perform high intensity magnetoelastic resonance and to be sensitive to changes in the media with the advantage of its reduced size. However, their size turned out to be just one of the improvements of microwire based sensors. In this work we present important features of the microwire magnetoelastic resonance that were overlooked in previous studies. The samples under study perform magnetoelastic resonance without any biasing field. The magnetoelastic response of those samples in the presence of a DC bias field depends dramatically on their magnetic properties. By means of temperature annealing, the microstructure of those microwires can be tailored via a nanocrystallization or crystallization process,<sup>29</sup> annealing temperature being the key factor to determine the final microstructure.

<sup>a)</sup> Author to whom correspondence should be addressed. Electronic mail: carlos.herrero.gomez@ucm.es. Tel.: +34913007173. FAX: +34913007176.

The experiments were performed on 30 mm length samples of amorphous magnetic microwires of composition  $Fe_{73}Si_{11}B_{13}Nb_3$  with 65 and 80  $\mu\text{m}$  of magnetic nucleus diameter and total diameter, respectively. The samples were subjected to 1 h heat treatments at the temperatures of 523, 623, 723, and 823 K in a nitrogen atmosphere. In addition to those four samples, the study of the resonance was also performed to an as-cast microwire sample and a 5 mm  $\times$  1 cm  $\times$  0.5 mm as cast METGLAS ribbon, in order to use the ribbon as a reference, and to compare it with the microwire results.

Measurements of the resonance frequency have been performed by using a magnetoelastic resonance analyzer set-up. The sample was placed inside a pick-up coil. The variation of the coil impedance with frequency allows the observation of the magnetoelastic resonance. The DC bias field, varying between  $-1000$  and  $1000$  A/m was produced by a Helmholtz coils system. The magnetic characterization was done by means of a Quantum Design Physical Property Measurement System (PPMS) equipped with a Vibrating Sample Magnetometer (VSM). Finally, it was tested a microwire as a magnetoelastic sensor by measuring the resonance of the as-cast sample under different media conditions and in the absence of any bias field. Two types of measurements were done, namely, a density sensor and a mass loading sensor.

Figure 1 represents the influence of DC bias magnetic field on the resonance spectrum for samples under study. The magnitude of the DC field was chosen so the resonance amplitude of the samples would vary between their maximum and minimum. The solid line represents the resonance in absence of applied field. Figure 1(a) shows the behavior of the amorphous ribbon. No resonance is observed in the absence of applied field. However, the sample resonates with maximum amplitude when a 500 A/m bias field is applied. It should also be highlighted that the sample response is the same for negative and positive applied fields, manifesting a symmetric behavior.

Figures 1(b) and 1(c) are very similar and correspond to the as-cast and 523 K annealed microwire, respectively. The observed behavior differs from the ribbon one. Contrary to the previous case, the biggest resonance is achieved without applied field. Increasing the field results in a lack of resonance

at 115 A/m for the as-cast sample and at 150 A/m for the 523 K annealed one.

Figure 1(d) represents the behavior of the 623 K annealed microwire. This sample also shows resonance without any applied field. However, in contrast to former samples, the application of a DC bias field may enhance the resonance amplitude. In addition to that effect, the bias field also generates a shift towards lower values of the resonance frequency. Finally, an application of a 140 A/m field totally cancels the resonance.

Figure 1(e) represents the 723 K annealed microwire whose response is similar to the 623 K annealed one.

Figure 2 shows the amplitude of the resonance peak for each of the samples as a function of the DC field. The three markers included correspond to the fields shown in Figure 1. The ribbon sample shown in Figure 2(a), which plays the role of the reference, shows the classical behavior for magnetoelastic resonance. The amplitude curve shows a symmetric broad dome shape with two maxima around  $\pm 500$  A/m.

The microwire amplitude vs field graph reveals a lack of symmetry with a systematic shift respect to the vertical axis. For the as-cast and the 523 K annealed sample, Figures 2(b) and 2(c), the behavior is similar to the one of the ribbon, but with the minimum shifted to a field around  $-115$  A/m. The resonance also vanishes for high values of the field modulus.

A huge change with respect to the previous cases is shown in Figures 2(d) and 2(e) which represent the 623 and 723 K annealed samples. The graph shows two narrow maxima instead of the broad dome shown by the ribbon and the as-cast and 523 annealed samples. Accordingly, the resonance vanishes for almost every applied field except for two particular regions of applied field around  $-100$  A/m and  $-200$  A/m. Finally, the 823 K annealed microwire does not show resonance for any applied field.

The evolution of the maximum amplitude of resonance in the absence of bias field as a function of the annealing temperature of the sample is shown in Fig. 3(a). This result can be used to deduce the optimal annealing temperature for the microwire to resonate. The figure clearly shows that there is an optimal temperature around 523 K for which the microwire undergoes the most intense resonance.

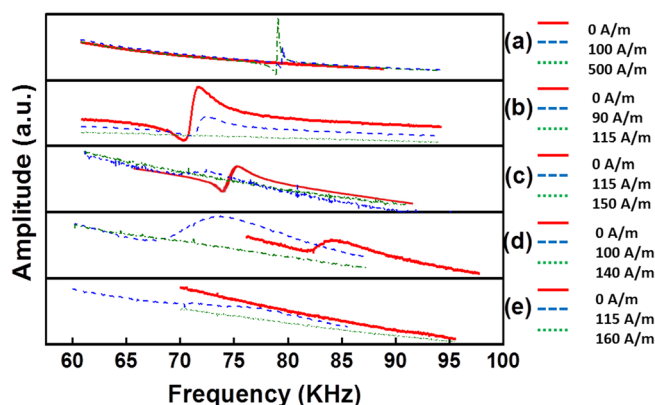


FIG. 1. Spectrum of resonance for three different values of applied DC field. (a) Metglas ribbon: 0, 100, and 500 A/m. (b) As cast microwire: 0, 90, and 115 A/m. (c) 523 K annealed microwire: 0, 115, and 150 A/m. (d) 623 K annealed microwire: 0, 100, and 140 A/m. (e) 723 K annealed microwire: 0, 115, and 160 A/m.

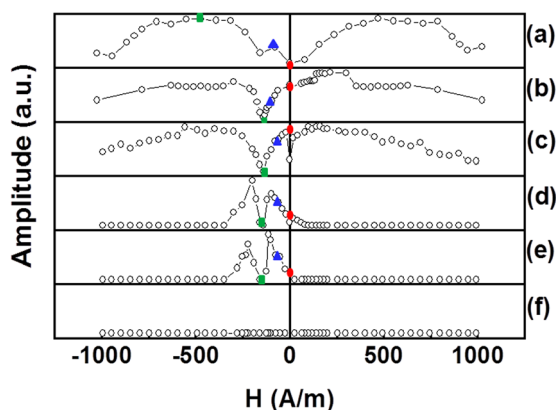


FIG. 2. Amplitude of resonance as a function of the applied DC field for the different samples. (a) Metglas ribbon, (b) as cast microwire, (c) 523 K annealed microwire, (d) 623 K annealed microwire, (e) 723 K annealed microwire, (f) 823 K annealed microwire. The symbols (square, triangle, and circle) remark the measurements corresponding to the spectra shown in Figure 1.

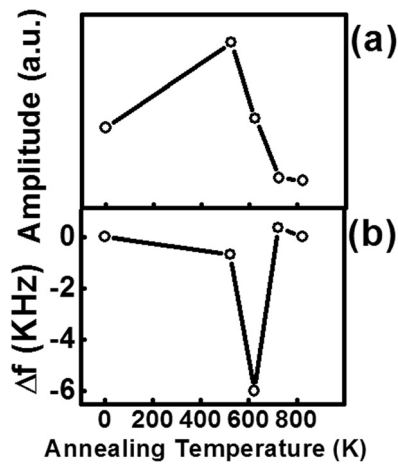


FIG. 3. (a) Amplitude of resonance in absence of bias field as a function of the microwire annealing temperature. (b) Frequency shift in the absence of bias field (difference between the resonance frequency of the as cast and annealed sample) as a function of the microwire temperature of annealing.

On the other hand, Figure 3(b) shows the frequency shift between the resonance frequency of the samples before and after being annealed in the absence of bias field. The maximum frequency shift, in absolute value, is achieved at about 623 K.

Figure 4 shows the hysteresis loops of the samples under study. On the upper panel the hysteresis loop between  $-5000$  and  $5000$  A/m is shown. The lower panel shows instead a closer look at the centre of the hysteresis loops. Figure 4(a) corresponds to the ribbon. The pattern displayed is a hysteresis-type loop presenting a transversal anisotropy with anisotropy field around  $H_k = 3500$  A/m. The as-cast wire, Figure 4(b), presents two regions with different susceptibilities that should be related with two well differentiated magnetization processes. The first region, from  $-250$  A/m to  $250$  A/m shows a bistable process from two states of magnetization between  $-0.25 M_s$  and  $0.25 M_s$  where  $M_s$  is saturation magnetization. As the applied field exceeds the  $250$  A/m the magnetization process towards saturation is similar to that observed in the case of the ribbon. The evolution of the loops as annealing temperature increases is as follows.

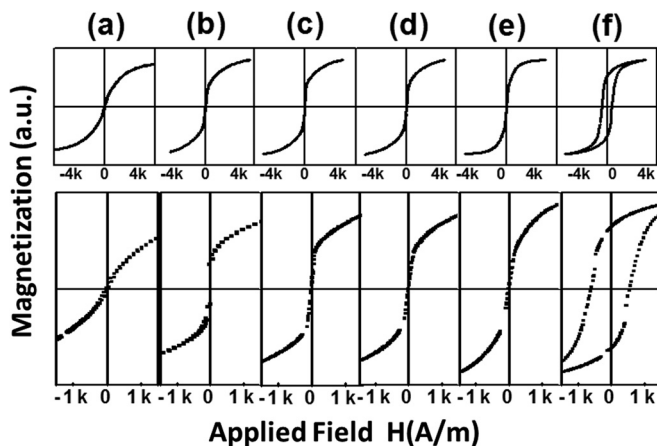


FIG. 4.  $-5000$ ,  $5000$  A/m hysteresis loop (upper panel).  $-1000$ ,  $1000$  A/m hysteresis loop (lower panel). (a) Metglas ribbon, (b) as cast microwire, (c)  $523$  K annealed microwire, (d)  $623$  K annealed microwire, (e)  $723$  K annealed microwire, (f)  $823$  K annealed microwire.

A loss of coercivity is observed for samples annealed at  $523$ ,  $623$ , and  $723$  K, respectively, although a high susceptibility central region remains in all cases. Furthermore, the sharp central magnetization jump observed for the as-cast and  $523$  K annealed samples, is smoothed as the annealing temperature increases. That is the consequence of the decrease of the anisotropy field achieved by means of the thermal annealing. Finally, the  $823$  K annealed sample shows hard magnetic behavior, associated with a high coercive field. Figure 5 illustrates how the aforementioned phenomena may be applied to develop different types of bias-free microwire-based magnetoelastic sensors. For that purpose, two samples of  $523$  K annealed microwire were immersed in different density media and loaded with different mass loads, respectively. The bias free magnetoelastic resonance was analysed in both cases and was compared with a control sensor of the same characteristics which was not immersed in liquid nor mass loaded. Figures 5(b) and 5(d) show the resonance spectrum as a function of the variation of the media parameter (density and mass load). Figures 5(a) and 5(c) show the effect of such variation in the amplitude and frequency resonance, compared with the control sensors. A clear dependence on the resonance parameters with both the mass load and liquid density is shown to appear. That suggests that such microwire based bias-free sensor arrangement may work properly as magnetoelastic sensor.

The magnetoelastic resonance is due to the rotation of the magnetization when a material is exposed to AC magnetic field of a certain frequency. An effective magnetoelastic coupling can only take place if several conditions are fulfilled at the same time. The first condition is a high value of magnetostriction constant ( $\lambda_s$ ) which basically depends on the material composition. This first condition is easily achieved by choosing Fe based alloys for the resonator. The second factor is closely related to the magnetic state of the material. In order to have magnetoelastic coupling the material should be magnetized but in a non-zero susceptibility state.<sup>30</sup> This is the case of the close-to-saturation region of a

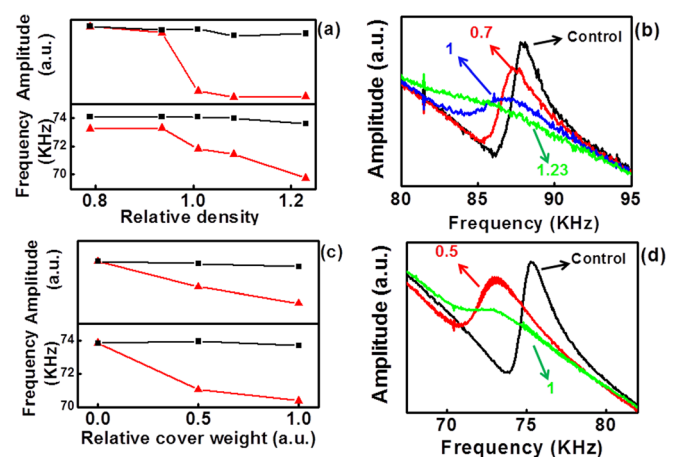


FIG. 5. Liquid density and mass load sensor test. (a) Amplitude and resonance frequency vs relative density for the sensing microwire (triangles) and a control microwire (squares). (b) Resonance spectra for different density of the media (control,  $0.7$ ,  $1$ , and  $1.2$  relative density). (c) Amplitude and resonance frequency vs cover weight (mass load) for the sensing microwire (triangles) and a control microwire (squares). (d) Resonance spectra for different cover weight (control,  $0.5$  and  $1$  of relative cover weight).



non bistable hysteresis loop. Usually a resonator is set into that magnetic state by means of the application of a DC bias field.

Amorphous alloys usually show smoothly curved hysteresis loops. In fact, in the case of the amorphous ribbons, any longitudinal anisotropy that may lead to some bistability can be eliminated by means of temperature annealing in presence of a transversal magnetic field.<sup>31</sup> Magnetoelastic resonance, can thus take place in those ribbons if a DC bias field is applied. That field value must be high enough to set the material in a magnetized state but low enough so the material is not saturated, which is consistent with Figure 2.

In contrast to the ribbons, that technique cannot be easily carried out in amorphous microwires. This is due to the presence of huge stresses in the radial direction which lead to very high values of anisotropy and a big axial domain. That axial domain leads to a bistable hysteresis loop. However, a good coupling factor for similar microwires has been obtained in a previous work,<sup>15</sup> by controlling the nanocrystalline fraction in the amorphous structure and decreasing that anisotropy.

The self-biasing magnetoelastic behavior observed in the microwires under study can be understood as follows. The observed hysteresis loops display two different regions, namely, a central nearly bistable region, and a smoother region close to saturation. This exotic behavior can be due to the coexistence of two types of magnetic structures: the aforementioned axial domain and some transverse anisotropy regions. The coexistence of those regions leads to a double effect. On the one hand, the transverse anisotropy and its associated smooth hysteresis behavior allows the magnetoelastic coupling since the magnetization is able to rotate. On the other hand, the axial domain plays the role of a bias field, magnetizing the material so no external field is needed to perform magnetoelastic resonance.

The temperature annealing also leads to two resulting effects. First, the material undergoes a stress relaxation process which implies a decrease of the longitudinal anisotropy. This effect is associated with barely hysteretic loops but which still preserve the self-biasing effect. That is shown to occur for temperatures lower than 823 K, when total crystallization happens. On the other hand, the temperature annealing also causes a partial nanocrystallization which increases the transversal anisotropy. Samples annealed at 623 and 723 K have a hysteresis loop that reaches saturation for lower values of applied fields. Those samples only perform magnetoelastic resonance for very concrete values of applied field, since for the rest of the values, the material is either demagnetized or saturated so that the magnetization vector cannot rotate.

We have concluded that amorphous microwires have unique features as magnetoelastic resonators. Such sensors have two main advantages. The first one is their reduced size compared with the ribbon-based sensors, a typical demand in state-of-the-art technology. The second advantage is the fact

of presenting free-bias magnetomechanical coupling which results in a free-bias magnetoelastic resonance. This feature is herein attributed to the coexistence of two different kinds of magnetic domains in the microwire.

This research was supported by the INNPACTO (IPT-2011-0893-420000) project from the Spanish ministry of economy and competitiveness. Authors want to acknowledge Vladimir Larin from MFTI Ltd. who kindly provided us with the microwire samples.

- <sup>1</sup>P. Marín, M. López, P. Agudo, M. Vázquez, and A. Hernando, *Sens. Actuators, A* **91**, 218–222 (2001).
- <sup>2</sup>M. Vázquez, in *Handbook of Magnetism and Advanced Magnetic Materials*, edited by H. Kronmüller and S. Parkin (Wiley, Chichester, UK, 2007), pp. 2193–2226.
- <sup>3</sup>H. Chiriac and D. Herea, *Int. J. Appl. Electrom.* **25**, 453–459 (2007).
- <sup>4</sup>K. Mhri and Y. Honkura, *Sens. Lett.* **5**, 267 (2007).
- <sup>5</sup>E. Kaniusas, L. Mehnen, and H. Pfützner, *J. Magn. Magn. Mater.* **254–255**, 624 (2003).
- <sup>6</sup>G. F. Taylor, *Phys. Rev.* **23**, 655–660 (1924).
- <sup>7</sup>S. A. Baranov, *Metal Sci. Heat Treat.* **43**(3–4), 167–168 (2001).
- <sup>8</sup>M. Vázquez and D. X. Chen, *IEEE Trans. Magn.* **34**, 724 (1998).
- <sup>9</sup>N. Vázquez, C. Gómez-Polo, D. X. Chen, and A. Hernando, *IEEE Trans. Magn.* **30**, 907 (1994).
- <sup>10</sup>P. Marín, M. Vázquez, J. Arcas, and A. Hernando, *J. Magn. Magn. Mater.* **203**, 6–11 (1999).
- <sup>11</sup>M. Vázquez, P. Marín, J. Arcas, A. Hernando, A. P. Zhukov, and J. González, *Textures Microstruct.* **32**, 245–267 (1999).
- <sup>12</sup>R. S. Beach and A. E. Berkowitz, *Appl. Phys. Lett.* **64**, 3652 (1994).
- <sup>13</sup>M. Vázquez and D. X. Chen, *IEEE Trans. Magn.* **31**, 1229–1238 (1995).
- <sup>14</sup>L. Kraus, G. Infante, Z. Frait, and M. Vázquez, *Phys. Rev. B* **83**, 174438 (2011).
- <sup>15</sup>P. Marín, M. Marcos, and A. Hernando, *Appl. Phys. Lett.* **96**, 262512 (2010).
- <sup>16</sup>C. A. Grimes, K. G. Ong, K. Loisel, P. G. Stoyanov, D. Kouzoudis, Y. Liu, C. Tong, and F. Tefiku, *Smart Mater. Struct.* **8**, 639 (1999).
- <sup>17</sup>C. A. Grimes, C. S. Mungle, K. Zeng, M. K. Jain, W. R. Dreschel, M. Paulose, and K. G. Ong, *Sensors* **2**, 294–313 (2002).
- <sup>18</sup>C. A. Grimes, S. C. Roy, S. Rani, and Q. Cai, *Sensors* **11**, 2809–2844 (2011).
- <sup>19</sup>M. Vázquez and A. Hernando, *J. Phys. D: Appl. Phys.* **29**, 939 (1996).
- <sup>20</sup>M. K. Jain, S. Schmidt, K. G. Ong, C. Mungle, and C. A. Grimes, *Smart Mater. Struct.* **9**, 502–510 (2000).
- <sup>21</sup>Q. Y. Cai, A. Cammers-Goodwin, and C. A. Grimes, *J. Environ. Monit.* **2**, 556 (2000).
- <sup>22</sup>Q. Y. Cai and C. A. Grimes, *Sens. Actuators B* **71**, 112 (2000).
- <sup>23</sup>L. G. Puckett, G. Barrett, D. Kouzoudis, C. A. Grimes, and L. G. Bachas, *Biosens. Bioelectron.* **18**, 675–681 (2003).
- <sup>24</sup>G. Rivero, M. Multigner, and J. Spottorno, “Magnetic Sensors for Biomedical Applications,” in *Magnetic Sensors*, edited by K. Kuang (InTech-Open Access Publisher, 2012), pp. 125–150.
- <sup>25</sup>X. Feng, S. C. Roy, G. K. Mor, and C. A. Grimes, *Sens. Lett.* **6**, 359–362 (2008).
- <sup>26</sup>C. A. Grimes and D. Kouzoudis, *Sens. Actuators, A* **84**, 205 (2000).
- <sup>27</sup>J. M. Barandiarán, J. Gutierrez, and C. Gómez-Polo, *Sens. Actuators, A* **81**, 154–157 (2000).
- <sup>28</sup>J. Gutierrez, J. M. Barandiarán, P. Mínguez, Z. Kaczowski, P. Ruuskanen, G. Vlasák, P. Svec, and P. Duhaj, *Sens. Actuators, A* **106**, 69–72 (2003).
- <sup>29</sup>M. Vázquez, P. Marín, H. A. Davies, and A. O. Olofinjana, *Appl. Phys. Lett.* **64**, 3184 (1994).
- <sup>30</sup>H. T. Savage and M. L. Spano, *J. Appl. Phys.* **53**, 8092 (1982).
- <sup>31</sup>C. Modzelewski, H. T. Savage, L. T. Kabacoff, and A. E. Clarck, *IEEE Trans. Magn.* **17**, 2837 (1981).